Foxp2 regulates anatomical features that may be relevant for vocal behaviors and bipedal locomotion

Shuqin Xu[a], Pei Liu[a], Yuanxing Chen[a], Yi Chen[b], Wei Zhang[a], Haixia Zhao[a], Yiwei Cao[a], Fuhua Wang[a], Nana Jiang[a], Shifeng Lin[a], Baojie Li[a], Zhenlin Zhang[c], Zhanying Wei[c], Ying Fan[c], Yunyun Jin[d], Lin He[a], Rujiang Zhou[a], Joseph D. Dekker[e], Haley O. Tucker[e], Simon E. Fisher[f,g], Zhengju Yao[a], Quansheng Liu[b,1], Xuechun Xia[a,1], and Xizhi Guo[a,1]

[a]Bio-X-Renji Hospital Research Center, Renji Hospital, School of Medicine, Shanghai Jiao Tong University, 200240 Shanghai, China; [b]Guangdong Key Laboratory of Animal Conservation and Resource Utilization, Guangdong Public Laboratory of Wild Animal Conservation and Utilization, Guangdong Institute of Applied Biological Resources, 510260 Guangzhou, China; [c]The Sixth People's Hospital of Shanghai, School of Medicine, Shanghai Jiao Tong University, 200240 Shanghai, China; [d]Institute of Biomedical Sciences and School of Life Sciences, East China Normal University, 200241 Shanghai, China; [e]Institute for Cellular and Molecular Biology, University of Texas at Austin, Austin, TX 78712; [f]Language and Genetics Department, Max Planck Institute for Psycholinguistics, Nijmegen 6525 XD, The Netherlands; and [g]Donders Institute for Brain, Cognition and Behaviour, Radboud University, Nijmegen 6500 HE, The Netherlands

Edited by Joseph S. Takahashi, Howard Hughes Medical Institute and University of Texas Southwestern Medical Center, Dallas, TX, and approved July 12, 2018 (received for review December 18, 2017)

Fundamental human traits, such as language and bipedalism, are associated with a range of anatomical adaptations in craniofacial shaping and skeletal remodeling. However, it is unclear how such morphological features arose during hominin evolution. FOXP2 is a brain-expressed transcription factor implicated in a rare disorder involving speech apraxia and language impairments. Analysis of its evolutionary history suggests that this gene may have contributed to the emergence of proficient spoken language. In the present study, through analyses of skeleton-specific knockout mice, we identified roles of ***Foxp2*** in skull shaping and bone remodeling. Selective ablation of ***Foxp2*** in cartilage disrupted pup vocalizations in a similar way to that of global ***Foxp2*** mutants, which may be due to pleiotropic effects on craniofacial morphogenesis. Our findings also indicate that Foxp2 helps to regulate strength and length of hind limbs and maintenance of joint cartilage and intervertebral discs, which are all anatomical features that are susceptible to adaptations for bipedal locomotion. In light of the known roles of Foxp2 in brain circuits that are important for motor skills and spoken language, we suggest that this gene may have been well placed to contribute to coevolution of neural and anatomical adaptations related to speech and bipedal locomotion.

Foxp2 | vocalization | bipedalism | cranial base | bone remodeling

S (1, 2). (3). 2 ( ) – (4–). *FOXP2* ( ) 3 *FOXP1*, *FOXP2*, (–11), *FOXP2* (12–14). 2 ( ) (1 –20), (21–23). 2

(24, 2). *FOXP2* (2 , 2). , *On the Origin of Species*, (2). 2 2 (2).

Significance

Speech and bipedalism are key aspects of behavior that emerged during human evolution. ***FOXP2***, a gene implicated in a human speech and language disorder, has been suggested to contribute to language evolution. Here, through knockout studies of mouse ***Foxp2***, we show that this gene is not only important for neural circuits involved in vocal behaviors, it also helps regulate relevant anatomical substrates. We additionally demonstrate that ***Foxp2*** influences skeletal features that may be relevant for bipedal locomotion. Our findings raise the possibility that ***FOXP2*** might be important for anatomical features contributing to derived human traits, including speech and bipedalism.

Author contributions: X.G. designed research; S.X., P.L., Yuanxing Chen, Yi Chen, W.Z., H.Z., Yiwei Cao, F.W., N.J., S.L., Y.J., R.Z., Z.Y., Q.L., and X.X. performed research; B.L., Z.Z., Z.W., Y.F., L.H., J.D.D., H.O.T., S.E.F., and Q.L. contributed new reagents/analytic tools; Q.L., X.X., and X.G. analyzed data; and X.G. wrote the paper.

The authors declare no conflict of interest.

This article is a PNAS Direct Submission.

[1]To whom correspondence may be addressed. Email: liuqs@giabr.gd.cn, xuechun.xia@sjtu.edu.cn, or xzguo2005@sjtu.edu.cn.

This article contains supporting information online at www.pnas.org/lookup/suppl/doi:10.1073/pnas.1721820115/-/DCSupplemental.

Published online August 13, 2018.

Foxp1/2 (30).

2

, -

, -

. , *Foxp2*

, (1 , 31).

, *Foxp2*

2 -

,

.

Results

Cartilage-Specific Deletion of *Foxp2*

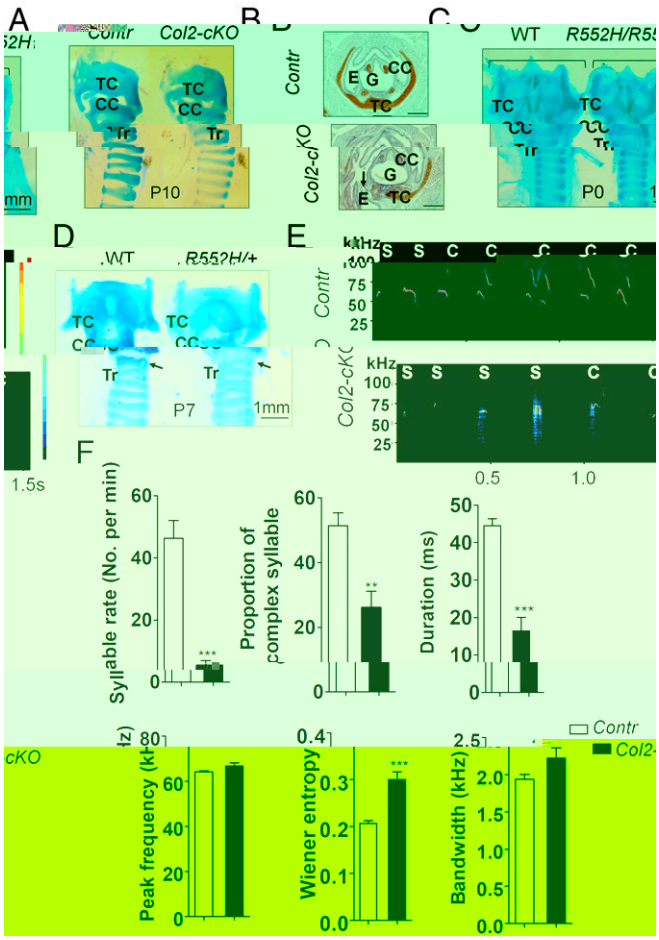

Fig. 2. Ablation of *Foxp2* in cartilage impairs USVs in pup calls. (*A*) Alcian blue staining of larynx cartilages from $Foxp2_{Col2}^{\Delta/\Delta}$ (*Col2-cKO*) mice. CC, cricoid cartilage; TC, thyroid cartilage; Tr, trachea cartilage. (*B*) Safranin O staining for the transverse sections of larynx at P10. (Scale bar, 500 μm.) E, esophagus; G, glottis. (*C* and *D*) Alcian blue staining of larynx cartilages from $Foxp2^{R552H/R552H}$ (*R552H/R552H*, *C*) at P0 and $Foxp2^{R552H/+}$ (*R552H/+*, *D*) mutant mice at P7. (*E*) Representative spectrograms of pup isolation calls in $Foxp2_{Col2}^{\Delta/\Delta}$ (*Col2-cKO*) mice at P10. The *y* axis indicates the frequency change of the USVs in the kilohertz range, whereas the *x* axis indicates time in seconds. Color depths in the sonograms represent relative intensity strength in decibels. C, complex syllable; S, simple syllable. (*F*) The sonic characteristics of pup calls, including syllable rate, proportion of complex syllables, syllable duration, peak frequency, wiener entropy, and bandwidth in $Foxp2^{fl/fl}$ (Contr) mice. $^*P < 0.05$; $^{**}P < 0.01$; $^{***}P < 0.001$. $Foxp2^{fl/fl}$ mice, $n = 27$; $Foxp2_{Col2}^{\Delta/\Delta}$ knockouts, $n = 26$.

(g. 2*E*). g
, $t(42) = -3.$ 1, $P < 0.01$, -
, $t(42) = 2.0$ 3, $P < 0.0$, g , $t(42) =$
.0 , $P < 0.01$, (g. 2*F*). g
. $Foxp1_{Col2}^{\Delta/\Delta}$
10 (*SI Appendix*, g. 4 *A B*). g
gg *Foxp2* g g
g , g g

Foxp2 Loss Perturbs Skull Integrity.

“ ” ,
g (34).
. 2

+ g
g ,
Osx-GFP:Cre 1 . (
SI Appendix, g. *A*). g
Foxp2 , g
Foxp2 g
g $Foxp2^{fl/fl}$ *Prx1-Cre* . $Foxp2_{Prx1}^{\Delta/\Delta}$
g g -
(*SI Appendix*, g. *B*), g
Foxp2 ( ) (*SI*
Appendix, g. *C D*). *Foxp2*
g g (g.
3*A*), +
(*SI Appendix*, g. *E*), g
g (*Osx*, *Runx2*, *Col1a1*, *Alp*) g
(*SI Appendix*, g. *F*).
$Foxp2^{R552H/R552H}$ $Foxp2^{R552H/+}$
(g. 3 *B C SI Appendix*, g.). -
$Foxp1/2_{Prx1}^{\Delta/\Delta}$ (g. 3*D*). g
gg 2 g g ,
g
, g g .

Ablation of *Foxp2* Impairs Leg Gracility and Cartilage Maintenance.

g , g ,
g , g
g . ,
$Foxp2_{Prx1}^{\Delta/\Delta}$
2 g (g. 4 *A B*).
- , 2 g
(*SI Appendix*, g. *A*). g
$Foxp2_{Prx1}^{\Delta/\Delta}$
, g -
g (*SI Appendix*, g. *B C*).
, g $Foxp2_{Prx1}^{\Delta/\Delta}$ -
g /
12 (g. 4*C*). , *Foxp2* -
g g ,
g .
Foxp2 -
g
(30), *Foxp2* g -
g .
g -

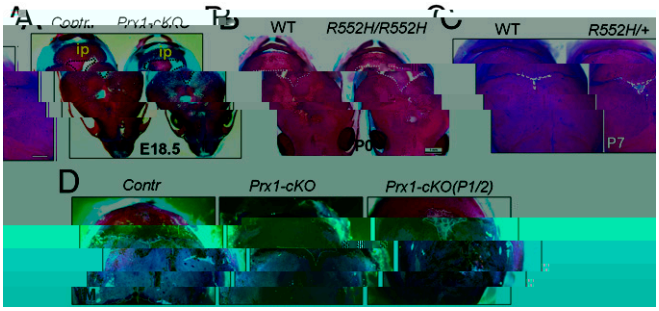

Fig. 3. Disruption of posterior skull integrity in *Foxp2* knockout mice. (*A*) Dorsal view of skulls of $Foxp2_{Prx1}^{\Delta/\Delta}$ mice (*Prx1-cKO*) at E18.5. Ip, interparietal bone. (*B* and *C*) Dorsal view of skulls of $Foxp2^{R552H/R552H}$ (*R552H/R552H*) mutant mice at P0 and $Foxp2^{R552H/+}$ mice (*R552H/+*) at P7. (*D*) Dorsal view of skulls of $Foxp1/2^{fl/fl}$, $Foxp2_{Prx1}^{\Delta/\Delta}$ (*Prx1-cKO*), and $Foxp1/2_{Prx1}^{\Delta/\Delta}$ [*Prx1-cKO* (*P1/2*)] mice at 1 mo of age. Dashed lines outline the lambdoid suture.

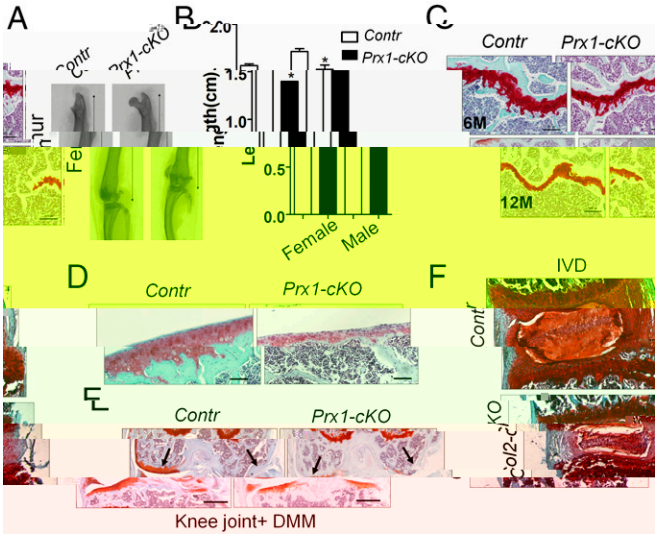

Fig. 4. Impaired articular cartilage integrity due to *Foxp2* loss. (*A*) Representative pictures of femur bones from *Foxp2*$^{fl/fl}$ (Contr) and *Foxp2*$_{Prx1}^{\Delta/\Delta}$ (*Prx1-cKO*) mice at 2 mo old. (*B*) Quantification of the length of femur bones in *A*. $n = 5$; $^{*}P < 0.05$. (*C*) Safranin O staining for growth plate in tibia bones from mice at 6 mo (*Upper*) and 12 mo (*Lower*) of age. (Scale bar, 500 μm.) (*D*) Representative pictures of articular cartilages from *Foxp2*$_{Prx1}^{\Delta/\Delta}$ (*Prx1-cKO*) mice at 6 mo of age. (*E*) Representative photographs of articular cartilages at knee joints from *Foxp2*$_{Prx1}^{\Delta/\Delta}$ (*Prx1-cKO*) 2-mo-old mice following 6-wk recovery from DMM surgery. (Scale bar, 100 μm.) (*F*) Representative pictures of intervertebral discs (IVDs) in lumbar vertebrates from *Foxp2*$_{Col2}^{\Delta/\Delta}$ (*Col2-cKO*) mice at 2 mo of age.

Foxp2$_{Prx1}^{\Delta/\Delta}$ ( )-
g , g
(g. 4*D*). g
( ) 2
g (g. 4*E*). g ,
( ) g
Foxp2$_{Col2}^{\Delta/\Delta}$ 2 g ,
(g. 4*F*).
g g gg
g (3).
g , g
.
Foxp2 g 2 g g
- g . g -
, *Foxp2*$_{Prx1}^{\Delta/\Delta}$
g ,
- (*SI Appendix*, g. *D*). g g-
g *Foxp2* g g g
. g ,
Foxp2 g g ,
g g g g g .

Foxp2 Regulates Bone Remodeling.

2 g g g, g
g, g -
- . *Foxp2*$_{Prx1}^{\Delta/\Delta}$ -
, μ ,
, , ,
2 g (g. *A* *SI Appendix*, g. *E*). & g
(*SI Appendix*, g. *F*).
Foxp2$_{Prx1}^{\Delta/\Delta}$,
g (*SI Appendix*, g. *G* *H*).
, g *Foxp2*-

, g (g. *B*), -
(*Alp*, *Col1a1*, *Runx2*,
Osterix *SI Appendix*, g. *A*) g g .
gg 2 g
.
. g g - -
Foxp2 g *Foxp2*$^{fl/fl}$ *Ctsk-Cre* .

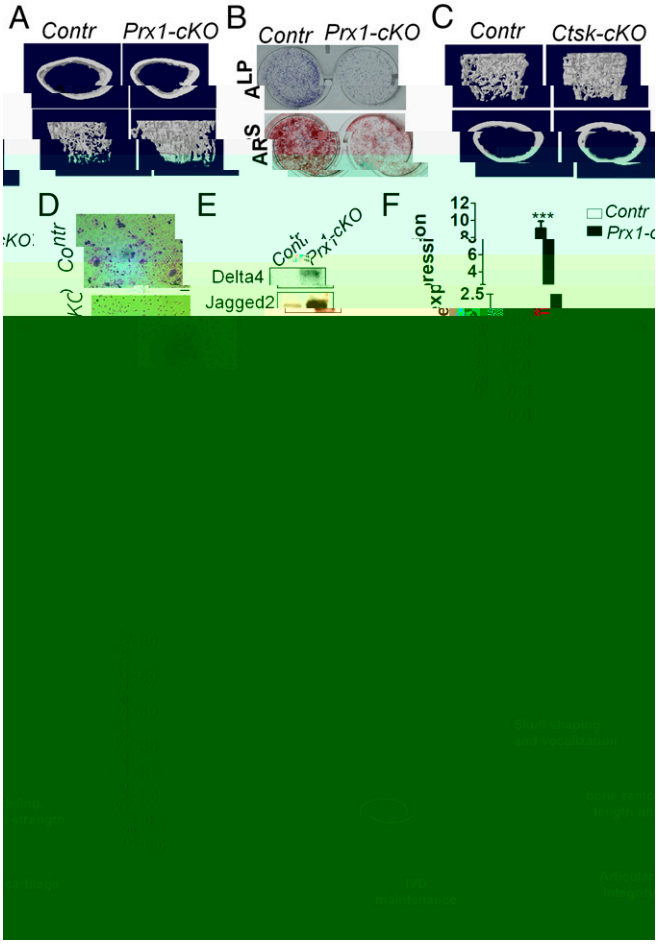

Fig. 5. Foxp2 controls bone remodeling in cooperation with Foxp1. (*A*) Representative images of 3D reconstruction of μCT analysis of *Foxp2*$_{Prx1}^{\Delta/\Delta}$ (*Prx1-cKO*) femur bones. (*Upper*) Cortical bone. (*Lower*) Trabecular bone. (*B*) ALP and Alizarin red staining following 14 d of osteogenic induction of MSCs from *Foxp2*$_{Prx1}^{\Delta/\Delta}$ (*Prx1-cKO*) mice at 2 mo of age. (*C*) Representative images of 3D reconstruction of μCT analysis of *Foxp2*$_{Ctsk}^{\Delta/\Delta}$ (*Ctsk-cKO*) femur bones at 2 mo of age. (*Upper*) Trabecular bone. (*Lower*) Cortical bone. (*D*) TRAP staining of osteoclastogenic cultures of bone marrow from *Foxp2*$_{Ctsk}^{\Delta/\Delta}$ (*Ctsk-cKO*) mice at 2 mo of age. (Scale bar, 250 μm.) (*E*) Western blotting detection of the expression of Notch-related proteins (Delta4, Jagged2, and Hey1) in MSCs from *Foxp2*$_{Prx1}^{\Delta/\Delta}$ (*Prx1-cKO*) mice. (*F*) qPCR assessment for expression of Notch-related marker genes (*Delta4*, *Jagged2*, *Hey1*, and *HeyL*) in bone marrow MSCs from *Foxp2*$_{Prx1}^{\Delta/\Delta}$ (*Prx1-cKO*) mice at 2 mo of age. $n = 3$. (*G* and *H*) Co-IP detected the in vivo interaction of Foxp1, Foxp2, and RBPjκ proteins in bone marrow MSCs, or in 293T cells transfected with the indicated plasmids. (*I*) Luciferase assay in 293T cells transfected with the indicated plasmids. Foxp2 repressed the transactivation of RBPjκ-Luc (containing RBPjκ DNA-binding sites in promoter region) by NICD2, whereas a Foxp2 missense mutation (R552H) alleviated the repressive function. $n = 3$. $^{*}P < 0.05$; $^{**}P < 0.01$; $^{***}P < 0.001$; ns, not significant. (*J*) Diagrammatic summaries of the pleiotropic roles of Foxp2 in helping to regulate anatomical features involved in vocalization and bone strengthening. Foxp2 regulates skull shaping, vocalization, and bone remodeling by forming complexes with Foxp1 and RBPjκ proteins.

Foxp2$_{Ctsk}^{\Delta/\Delta}$ 2 g (g. *C* *SI Appendix*, g. *C*). *Foxp2*$_{Ctsk}^{\Delta/\Delta}$ ( ) g (g. *D*). - g g (*c-Fos*, *Nfat2*, *Ctsk*, *Trap*, *Rankl*) (*SI Appendix*, g. *B*). gg 2 . 2 g g g .

Foxp2 Controls Bone Formation in Cooperation with Foxp1. *Foxp1* *Foxp2* (g. 3*D* *SI Appendix*, g. 2). 1 g g g g (3). *Foxp2*$_{Prx1}^{\Delta/\Delta}$ g g (.g., 4, g2, g1, 1, g. *E* *F*). , *Foxp1/2*$_{Prx1}^{\Delta/\Delta}$ *Foxp1* *Foxp2* g (*SI Appendix*, g.). 2 1 κ , g (-) (g. *G* *H*). 2 *Rbpjκ-Luc* (2), 2 (2) - g (g. *I*). gg 2, 1, g g g.

Discussion

, g g g g (3). 2 g g . g. *J*, gg 2 - g g (*i*) g, g (*ii*) g , g g , (*iii*) g g , g g . , 2 - g , , . g g g *FOXP2* (. ., - g), g g (3 , 3). , g *Foxp2* g g g (40–42). g *FOXP2* (3). - g , g ( ), g g / g . g g *FOXP2* (43). / g *FOXP2* - . g , *FOXP2* (12, 13, 44, 4), g g g . , g - *Foxp2* , (*SI Appendix*, g. 10). g g - 2. , - g (4), 2 , *Foxp2*^{R552H} g - g , g g g (*SI Appendix*, g . 1 3). - g g g g g . g (33). , - , g g g . - , g g g (4). g g g , g g . , g - *Foxp2* - , (g. 2*A*–*D*). , *Foxp1*$_{Col2}^{\Delta/\Delta}$ *Foxp2*$_{Col2}^{\Delta/\Delta}$ (g. 2*F* *SI Appendix*, g. 4*B*). , , g - g (4 , 4), g - *Foxp1*$_{Col2}^{\Delta/\Delta}$, *Foxp2*$_{Col2}^{\Delta/\Delta}$. g g (0). *FOXP1* *FOXP2* g , g g g (11). g *FOXP1* , g g , , , , (, 1). g , - *Foxp1* (2, 3). , g - *Foxp1* , *Foxp2*. , *Foxp1* *Foxp2* - g (g. 3 *SI Appendix*, g . 2 *F* *G*). , 1 2 g g. g g g g (3). g *FOXP2* g , g g , g - (24, 2). g g , g g g g g (3 , 4). g - g g (1), g 2 . g , g gg 2 g . , 2 g g g (g. 3), , g ( ). , 2 g g g

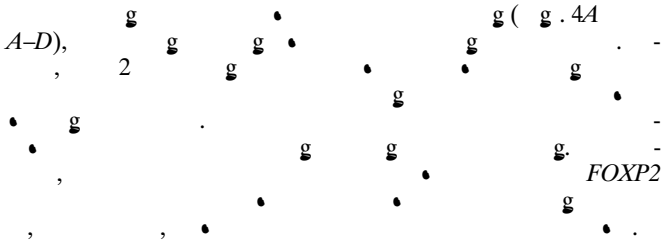

A–D),

FOXP2

Materials and Methods

All animal experiments were performed according to the guidelines and approved by the ethical committee of Bio-X Institutes of Shanghai Jiao Tong University (SYXK 2011-0112). For skeletal morphological analysis, skeletal preparations for mice of different ages were made by Alcian blue/Alizarin red staining as previously reported. For μCT analysis, femurs were dissected from mice and fixed in 70% ethanol at 4 °C. μCT scanning of bones was performed on SkyScan 1176. A 3D model was reconstructed and structural indices were calculated using CTAn software, and the region of interest selected was 5 mm below growth plate of bones.

The details of other materials and methods can be found in *SI Appendix*.

ACKNOWLEDGMENTS. We are grateful to Prof. Jianquan Chen in Suzhou University for μCT scanning. This work was supported by research funding from National Major Fundamental Research 973 Program of China Grant 2014CB942902 and National Natural Science Foundation of China Grants 91749103, 81421061, 31100624, and 81200586 (to X.G.); Project of Comprehensive Strategic Cooperation between Guangdong Province and the Chinese Academy of Sciences Grant 2012B091100260 and Guangdong Academy of Sciences Grants 2016GDASPT-0215 and 2017GDASCX-0107 (to Q.L.); NIH Grant R01CA31534; Cancer Prevention Research Institute of Texas Grants RP120348 and RP120459; the Marie Betzner Morrow Centennial Endowment (to H.O.T.); and Lymphoma Research Foundation Award 300463 (to J.D.D.). S.E.F. is supported by the Max Planck Society.

1. Boeckx C, Benítez-Burraco A (2015) Osteogenesis and neurogenesis: A robust link also for language evolution. *Front Cell Neurosci* 9:291.
2. Neubauer S, Hublin JJ, Gunz P (2018) The evolution of modern human brain shape. *Sci Adv* 4:eaao5961.
3. Deriziotis P, Fisher SE (2017) Speech and language: Translating the genome. *Trends Genet* 33:642–656.
4. Vargha-Khadem F, Watkins K, Alcock K, Fletcher P, Passingham R (1995) Praxic and nonverbal cognitive deficits in a large family with a genetically transmitted speech and language disorder. *Proc Natl Acad Sci USA* 92:930–933.
5. Watkins KE, Dronkers NF, Vargha-Khadem F (2002) Behavioural analysis of an inherited speech and language disorder: Comparison with acquired aphasia. *Brain* 125: 452–464.
6. Lai CS, Fisher SE, Hurst JA, Vargha-Khadem F, Monaco AP (2001) A forkhead-domain gene is mutated in a severe speech and language disorder. *Nature* 413:519–523.
7. Morgan A, Fisher SE, Scheffer I, Hildebrand M (2016) *FOXP2*-related speech and language disorders. Available at https://www.ncbi.nlm.nih.gov/pubmed/27336128. Accessed July 26, 2018.
8. Pariani MJ, Spencer A, Graham JM, Jr, Rimoin DL (2009) A 785kb deletion of 3p14.1p13, including the FOXP1 gene, associated with speech delay, contractures, hypertonia and blepharophimosis. *Eur J Med Genet* 52:123–127.
9. Carr CW, et al. (2010) Chiari I malformation, delayed gross motor skills, severe speech delay, and epileptiform discharges in a child with FOXP1 haploinsufficiency. *Eur J Hum Genet* 18:1216–1220.
10. Sollis E, et al. (2016) Identification and functional characterization of de novo FOXP1 variants provides novel insights into the etiology of neurodevelopmental disorder. *Hum Mol Genet* 25:546–557.
11. Sollis E, et al. (2017) Equivalent missense variant in the FOXP2 and FOXP1 transcription factors causes distinct neurodevelopmental disorders. *Hum Mutat* 38:1542–1554.
12. Turner SJ, et al. (2013) Small intragenic deletion in FOXP2 associated with childhood apraxia of speech and dysarthria. *Am J Med Genet A* 161A:2321–2326.
13. Reuter MS, et al.; DDD Study (2017) FOXP2 variants in 14 individuals with developmental speech and language disorders broaden the mutational and clinical spectrum. *J Med Genet* 54:64–72.
14. Estruch SB, Graham SA, Chinnappa SM, Deriziotis P, Fisher SE (2016) Functional characterization of rare FOXP2 variants in neurodevelopmental disorder. *J Neurodev Disord* 8:44.
15. Kurt S, Fisher SE, Ehret G (2012) Foxp2 mutations impair auditory-motor association learning. *PLoS One* 7:e33130.
16. Shu W, et al. (2005) Altered ultrasonic vocalization in mice with a disruption in the Foxp2 gene. *Proc Natl Acad Sci USA* 102:9643–9648.
17. Fujita E, et al. (2008) Ultrasonic vocalization impairment of Foxp2 (R552H) knockin mice related to speech-language disorder and abnormality of Purkinje cells. *Proc Natl Acad Sci USA* 105:3117–3122.
18. Fujita-Jimbo E, Momoi T (2014) Specific expression of FOXP2 in cerebellum improves ultrasonic vocalization in heterozygous but not in homozygous Foxp2 (R552H) knock-in pups. *Neurosci Lett* 566:162–166.
19. Gaub S, Fisher SE, Ehret G (2016) Ultrasonic vocalizations of adult male Foxp2-mutant mice: Behavioral contexts of arousal and emotion. *Genes Brain Behav* 15:243–259.
20. Chabout J, et al. (2016) A Foxp2 mutation implicated in human speech deficits alters sequencing of ultrasonic vocalizations in adult male mice. *Front Behav Neurosci* 10:197.
21. Miller JE, et al. (2008) Birdsong decreases protein levels of FoxP2, a molecule required for human speech. *J Neurophysiol* 100:2015–2025.
22. Schulz SB, Haesler S, Scharff C, Rochefort C (2010) Knockdown of FoxP2 alters spine density in area X of the zebra finch. *Genes Brain Behav* 9:732–740.
23. Murugan M, Harward S, Scharff C, Mooney R (2013) Diminished FoxP2 levels affect dopaminergic modulation of corticostriatal signaling important to song variability. *Neuron* 80:1464–1476.
24. Enard W, et al. (2002) Molecular evolution of FOXP2, a gene involved in speech and language. *Nature* 418:869–872.
25. Coop G, Bullaughey K, Luca F, Przeworski M (2008) The timing of selection at the human FOXP2 gene. *Mol Biol Evol* 25:1257–1259.
26. Enard W, et al. (2009) A humanized version of Foxp2 affects cortico-basal ganglia circuits in mice. *Cell* 137:961–971.
27. Schreiweis C, et al. (2014) Humanized Foxp2 accelerates learning by enhancing transitions from declarative to procedural performance. *Proc Natl Acad Sci USA* 111:14253–14258.
28. Ghazanfar AA, Rendall D (2008) Evolution of human vocal production. *Curr Biol* 18: R457–R460.
29. Konopka G, et al. (2009) Human-specific transcriptional regulation of CNS development genes by FOXP2. *Nature* 462:213–217.
30. Zhao H, et al. (2015) Foxp1/2/4 regulate endochondral ossification as a suppresser complex. *Dev Biol* 398:242–254.
31. Chen YC, et al. (2016) Foxp2 controls synaptic wiring of corticostriatal circuits and vocal communication by opposing Mef2c. *Nat Neurosci* 19:1513–1522.
32. Lieberman DE, McBratney BM, Krovitz G (2002) The evolution and development of cranial form in Homosapiens. *Proc Natl Acad Sci USA* 99:1134–1139.
33. Fitch WT (2000) The evolution of speech: A comparative review. *Trends Cogn Sci* 4: 258–267.
34. Esteve-Altava B, Rasskin-Gutman D (2015) Evo-devo insights from pathological networks: Exploring craniosynostosis as a developmental mechanism for modularity and complexity in the human skull. *J Anthropol Sci* 93:103–117.
35. Bramble DM, Lieberman DE (2004) Endurance running and the evolution of Homo. *Nature* 432:345–352.
36. Li H, et al. (2017) FOXP1 controls mesenchymal stem cell commitment and senescence during skeletal aging. *J Clin Invest* 127:1241–1253.
37. Konopka G, Roberts TF (2016) Insights into the neural and genetic basis of vocal communication. *Cell* 164:1269–1276.
38. Fisher SE, Scharff C (2009) FOXP2 as a molecular window into speech and language. *Trends Genet* 25:166–177.
39. Vargha-Khadem F, Gadian DG, Copp A, Mishkin M (2005) FOXP2 and the neuroanatomy of speech and language. *Nat Rev Neurosci* 6:131–138.
40. French CA, et al. (2012) An aetiological Foxp2 mutation causes aberrant striatal activity and alters plasticity during skill learning. *Mol Psychiatry* 17:1077–1085.
41. Vernes SC, et al. (2011) Foxp2 regulates gene networks implicated in neurite outgrowth in the developing brain. *PLoS Genet* 7:e1002145.
42. Groszer M, et al. (2008) Impaired synaptic plasticity and motor learning in mice with a point mutation implicated in human speech deficits. *Curr Biol* 18:354–362.
43. Schulze K, Vargha-Khadem F, Mishkin M (2018) Phonological working memory and FOXP2. *Neuropsychologia* 108:147–152.
44. Feuk L, et al. (2006) Absence of a paternally inherited FOXP2 gene in developmental verbal dyspraxia. *Am J Hum Genet* 79:965–972.
45. Rice GM, et al. (2012) Phenotype of FOXP2 haploinsufficiency in a mother and son. *Am J Med Genet A* 158A:174–181.
46. Haesler S, et al. (2007) Incomplete and inaccurate vocal imitation after knockdown of FoxP2 in songbird basal ganglia nucleus area X. *PLoS Biol* 5:e321.
47. Mahrt E, Agarwal A, Perkel D, Portfors C, Elemans CP (2016) Mice produce ultrasonic vocalizations by intra-laryngeal planar impinging jets. *Curr Biol* 26:R880–R881.
48. Elemans CP, et al. (2015) Universal mechanisms of sound production and control in birds and mammals. *Nat Commun* 6:8978.
49. Riede T (2011) Subglottal pressure, tracheal airflow, and intrinsic laryngeal muscle activity during rat ultrasound vocalization. *J Neurophysiol* 106:2580–2592.
50. French CA, Fisher SE (2014) What can mice tell us about Foxp2 function? *Curr Opin Neurobiol* 28:72–79.
51. Song H, Makino Y, Noguchi E, Arinami T (2015) A case report of de novo missense FOXP1 mutation in a non-Caucasian patient with global developmental delay and severe speech impairment. *Clin Case Rep* 3:110–113.
52. Usui N, et al. (2017) Foxp1 regulation of neonatal vocalizations via cortical development. *Genes Dev* 31:2039–2055.